

SEAL: Semantic Aware Image Watermarking

Kasra Arabi, R. Teal Witter, Chinmay Hegde, Niv Cohen
New York University

Abstract

Generative models have rapidly evolved to generate realistic outputs. However, their synthetic outputs increasingly challenge the clear distinction between natural and AI-generated content, necessitating robust watermarking techniques. Watermarks are typically expected to preserve the integrity of the target image, withstand removal attempts, and prevent unauthorized replication onto unrelated images. To address this need, recent methods embed persistent watermarks into images produced by diffusion models using the initial noise. Yet, to do so, they either distort the distribution of generated images or rely on searching through a long dictionary of used keys for detection.

In this paper, we propose a novel watermarking method that embeds semantic information about the generated image directly into the watermark, enabling a distortion-free watermark that can be verified without requiring a database of key patterns. Instead, the key pattern can be inferred from the semantic embedding of the image using locality-sensitive hashing. Furthermore, conditioning the watermark detection on the original image content improves robustness against forgery attacks. To demonstrate that, we consider two largely overlooked attack strategies: (i) an attacker extracting the initial noise and generating a novel image with the same pattern; (ii) an attacker inserting an unrelated (potentially harmful) object into a watermarked image, possibly while preserving the watermark. We empirically validate our method’s increased robustness to these attacks. Taken together, our results suggest that content-aware watermarks can mitigate risks arising from image-generative models. Our code is available at <https://github.com/Kasraarabi/SEAL>.

1. Introduction

The growing capabilities of generative models pose risks to society, including misleading public opinion, violating privacy or intellectual property, and fabricating legal evidence [5, 14, 22]. Watermarking methods aim to mitigate such risks by allowing the detection of generated contents.

Yet, many conventional watermarking techniques lack

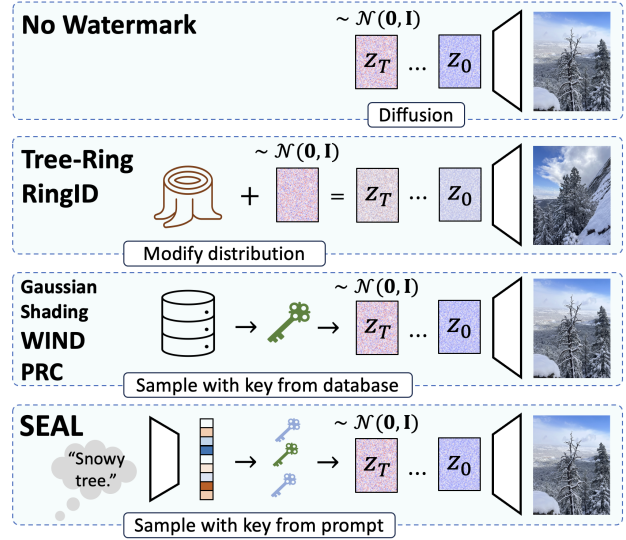


Figure 1. **Illustration of different watermarking frameworks using the initial noise of diffusion models.** **No Watermark:** A diffusion model maps pure Gaussian noise to an image. **Tree-Ring:** A pattern is added to the initial noise, modifying the distribution of generated images in a detectable way. **Key-Based Watermarking:** A key is sampled to generate distortion-free images linked to the key. **Ours (SEAL):** The initial noise is conditioned on multiple keys derived from the image’s semantic embedding, with each key influencing a different patch.

robustness against adversaries who attempt to remove them using regeneration attacks powered by recent generative models [9, 18, 24]. To address this, new watermarking techniques leveraging advances in generative models offer increased robustness against such attacks [4, 25, 27]. Namely, these methods embed a watermarking pattern in the initial noise used by a diffusion model. These patterns have been shown to be more robust against existing removal attacks.

However, existing watermarks that utilize the diffusion model initial noise tend to be vulnerable to other attacks aiming to “steal” the watermark and apply it to images unrelated to the watermark owners. Some of these *watermark forgery* attacks can be evaded by using a distortion-free watermark-generating watermarked images from a similar distribution

to the distribution of non-watermarked images; therefore exposing less information about the watermark identity. Even so, using an extensively large number of watermark identities requires maintaining a database of used noises, and might still be forgeable by other attacks.

To address these challenges, we introduce SEAL - *Semantic Embedding for AI Lineage*, a method that embeds watermark patterns directly tied to image semantics. Our approach enables direct watermark detection from image samples and offers the following key properties: (i) *Distortion-free*: As in previous works, we utilize pseudo-random hash functions to generate an initial noise that is similar to the noise used by non-watermarked models, ensuring a similar distribution of generated images. (ii) *Robust to regeneration attacks*: Similar to prior watermarking methods based on DDIM inversion, our approach demonstrates resilience against regeneration-based removal attempts [28]. (iii) *Correlated with image semantics*: The applied watermark encodes semantic information from the image. (iv) *Independent of a historical database*: Unlike previous methods that rely on a database of past generations, our approach embeds watermarks without requiring access to such a database, making detection possible without prior stored data.

Our key insight is that we can encode semantic information about the image content in a distortion-free watermark by embedding the semantic encoding directly into the initial noise. We use projections of the user prompt embedding to seed different pseudo-random patches that compose the initial noise. We ensure the encoded embedding correlates strongly with the resulting image content, not just with the prompt, which is important since the prompt is not available during detection. At detection time, our approach identifies an image as watermarked only when the watermark pattern is both present and properly correlated with the image semantics. We describe in detail our watermarking technique in Section 3.

Correlating our watermarking algorithm to the image semantics also allows us to resist forgery attacks that are challenging for many existing approaches. An attacker attempting to forge such a watermark onto unauthorized content would alter the image’s semantic embedding, breaking its correlation with the embedded pattern and rendering the watermark invalid.

One mostly overlooked attack involves an adversary altering only small portions of a watermarked image while preserving the rest of its content. In such cases, the attacker can manipulate the image to be offensive, illegal, or damaging to the watermark owner’s reputation, all while the original watermark remains detectable. We term this attack the CAT ATTACK, as the attacker may add an object to the image (e.g., a cat) and expect the watermark to persist. We evaluate the potential damage of such attacks and demonstrate that our method uniquely provides robustness against

both the CAT ATTACK and forgery attempts by adversaries who obtain accurate copies of our initial noise. Our experiments confirm our method’s effectiveness against these novel threats as well as previously studied attack vectors.

Our contributions are as follows:

- We propose SEAL, a semantic-aware database-free watermarking method that integrates image semantics into the watermark, ensuring it becomes invalid under severe semantic changes.
- We identify the CAT ATTACK, highlighting the risks of local edits to watermark owners and assessing their potential impact.
- We empirically demonstrate the effectiveness of our watermark against various attacks, including its resistance to adversarial edits.

2. Related works

Recent research on image watermarking can be broadly categorized into post-processing and in-processing approaches, each offering distinct trade-offs between quality, robustness, and deployment practicality [2]. We cover here *In-Processing Methods*, and for *Post-Processing Methods* refer to Appendix 8.

In-Processing Methods. In-processing approaches integrate watermark embedding directly within the image generation process. These methods are often used in diffusion models to achieve minimal perceptual impact. Some methods modify the generative model entirely by fine-tuning specific components, as demonstrated in Stable Signature [10]. An alternative class of techniques manipulates the initial noise of the generation process, thereby embedding the watermark without extensive model retraining. For example, Tree-Ring [25] embeds a Fourier-domain pattern into the initial noise, which can be detected through DDIM inversion [23], while RingID [7] extends this idea to support multiple keys. Other notable methods include Gaussian Shading, which produces a unique key for each watermark owner [27], PRC that leverages pseudo-random error-correcting codes for computational undetectability [12], and WIND, which employs a two-stage detection process to enable a very large number of keys [4].

Locally Sensitive Hashing in High-Dimensional Spaces.

Recent advances in approximate nearest neighbor (ANN) search have increasingly relied on the power of Locally Sensitive Hashing (LSH) to address the challenges inherent in high-dimensional data. Originally introduced by Indyk and Motwani [13] and further refined by Gionis et al. [11], LSH employs randomized hash functions that ensure similar data points are mapped to the same bucket with high probability. Formally, for a hash family \mathcal{H} , the collision probability is

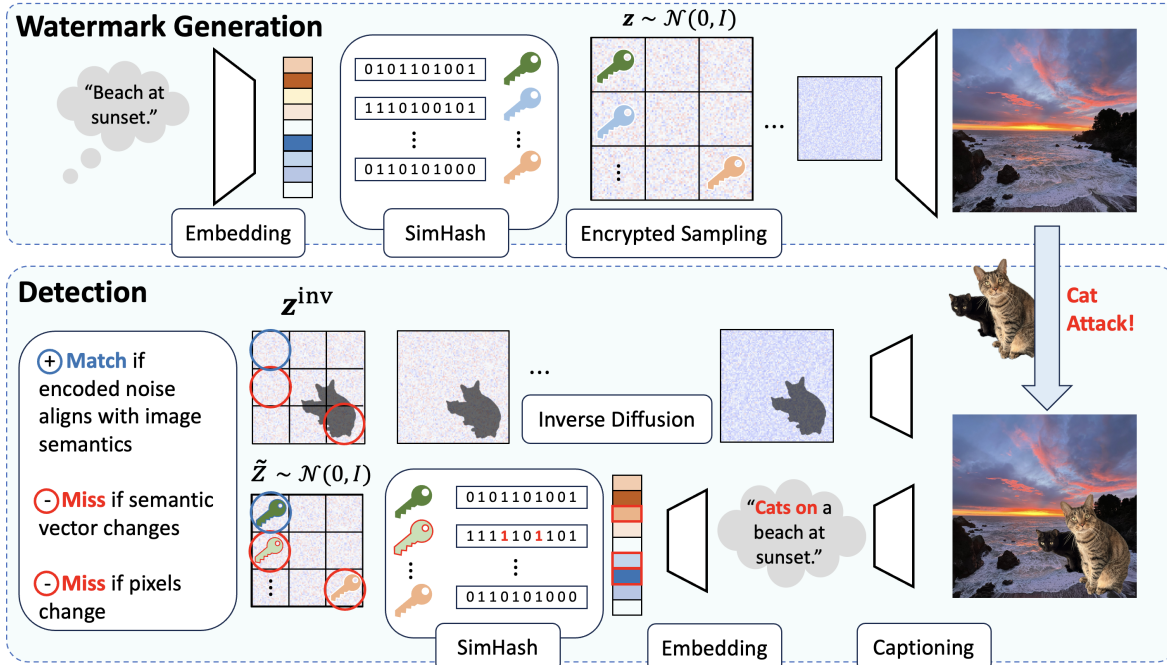


Figure 2. *Illustration of the SEAL watermarking framework for diffusion models using semantic-aware noise patterns. Watermark Generation:* A textual prompt (e.g., “Beach at sunset.”) is first embedded into a semantic space. The embedding is then processed using *SimHash* to generate discrete keys, which are used in *Encrypted Sampling* to choose the initial noise $\mathbf{z} \sim \mathcal{N}(0, I)$. The watermarked noise then undergoes standard diffusion to generate the final image. *Detection:* The image is captioned to obtain an embedding, which is then processed by *SimHash* to generate a reference noise, similar to watermark generation. This noise remains correlated with the initial noise used during generation as long as the image semantics remain unchanged. The image is also processed through *Inverse Diffusion* to estimate the actual initial noise used during its generation. If there are insufficient matches between the reference noise and the noise obtained from inversion, the watermarking framework flags the image as non-watermarked. If a key match is found but the image is still deemed suspicious, a detailed inspection of the patches can be performed to identify local edits.

given by

$$P(h(x) = h(y)) \approx \text{similarity}(x, y), \quad h \in \mathcal{H}.$$

Subsequent improvements by Datar et al. [8] and Andoni and Indyk [3] have enhanced both the efficiency and robustness of LSH methods, making them key for large-scale, high-dimensional search tasks.

3. SEAL: Semantic Aware Watermarking

3.1. Motivation

Watermarking methods suffer from an inherent trade-off: a watermark that is harder to remove is also easier to attach to unrelated generations, compromising the reputation of the watermark owner [5]. One suggested solution to overcome this trade-off, might be maintaining a database of past generations, such that the owner could compare a seemingly watermarked image to the actual past generations. Yet, this solution is not without its problems. First, maintaining and searching a rapidly growing database, which expands with each new generation, can be challenging. Second, safeguard-

ing the database itself may pose security risks. Finally, in various use cases, the watermark owner may not only wish to detect if an image is watermarked but also provide to a third party evidence that it is. We therefore turn to suggest a watermarking scheme that is hard to remove, hard to forge, and does not rely on maintaining a database of past generations.

Our core idea is to use a distortion-free initial noise pattern not only to indicate the origin of the image but also to encode which semantic information the image may contain. We do so in three stages (see also Figure 2): (i) Semantic Embedding – we predict a vector representing the expected semantic content in each generated image (ii) SimHash Encoding – we encode the semantic vector using a set of multi-bit hash functions (iii) Encrypted Sampling – The pseudo-random outputs of these functions are combined to produce the initial noise for the denoising process. Taken together, these steps set an initial noise that is both distortion-free with respect to standard random initialization and correlated with the semantics of the input prompt (see Section 3.3). We describe our watermarking method in detail below.

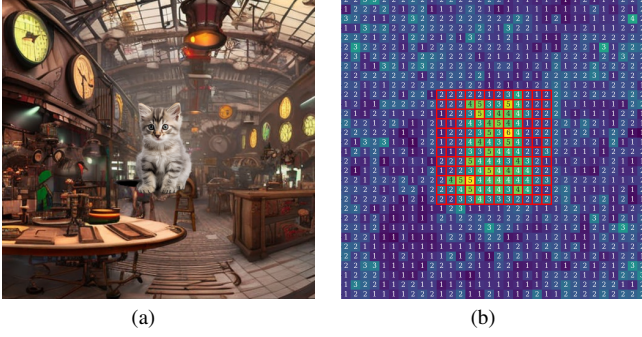


Figure 3. *Effect of the Cat Attack on SEAL.* (Left) A cat image is pasted onto a watermarked image at a random position and scale. (Right) Our method detects this modification by identifying elevated ℓ_2 norms in affected patches.

3.2. Method

Formally, our method first creates a semantic vector \mathbf{v} and uses it to sample the initial noise \mathbf{z} for the watermarked image. During detection, we aim to verify the connection between the used initial noise \mathbf{z} and the semantic embedding of the image. When approximating \mathbf{z} from the generated image during detection and verifying it, we consider the following error sources:

- We do not have access to \mathbf{v} at detection time; instead, we must use an approximate version $\tilde{\mathbf{v}}$ derived from the image we’re analyzing. Using $\tilde{\mathbf{v}}$, we produce an approximate version of the used initial noise $\tilde{\mathbf{z}}$.
- Because of the randomness in the diffusion process and its inversion, we cannot reproduce exactly \mathbf{z} ; instead, we reconstruct noise from the suspect image to obtain the inverted noise \mathbf{z}^{inv} .

We would ideally like for \mathbf{z}^{inv} to align with $\tilde{\mathbf{z}}$ but this is not guaranteed because both differ from \mathbf{z} due to the error sources mentioned above. Instead, we separate each noise vector into patches and compare them. Our method provides a high likelihood that even if some patches do not match because of the challenges discussed above, many of the patches will match as long as the suspect image is watermarked.

Semantic Patterns with SimHash

The core subroutine of our watermarking method is SimHash [6], used to generate initial noise maps correlated to a given vector (Algorithm 1). SimHash takes a vector \mathbf{v} and generates an initial noise \mathbf{z}_i for patch i , allowing a verifier to later determine, with some probability, whether \mathbf{z}_i is related to \mathbf{v} . Namely, the semantic vector \mathbf{v} is passed through a locality-sensitive hashing method that generates representations of \mathbf{v} in terms of its projections in random directions.

Specifically, SimHash projects \mathbf{v} onto a set of random vectors. The input to the hash function is determined by the

Algorithm 1 SimHash

- 1: **Input:** \mathbf{v} : semantic vector, i : patch index, salt: secret salt, b : number of bits, hash: cryptographic hash function
 - 2: **Output:** Semantic, secure, normally distributed noise
 - 3: $\text{bits} \leftarrow \mathbf{0}$ // Initialize hash input
 - 4: **for** $j = 1, \dots, b$ **do**
 - 5: // Reproducibly sample random vector
 - 6: $s \leftarrow \text{hash}(i, j, \text{salt})$
 - 7: Sample $\mathbf{r}_j^{(i)} \stackrel{s}{\sim} \mathcal{N}(\mathbf{0}, \mathbf{I})$
 - 8: $\text{bits}[j] \leftarrow \text{sign}(\langle \mathbf{v}, \mathbf{r}_j^{(i)} \rangle)$ // Random projection
 - 9: **end for**
 - 10: $s_i \leftarrow \text{hash}(\text{bits}, i, \text{salt})$
 - 11: **return** $\mathbf{z}_i \stackrel{s_i}{\sim} \mathcal{N}(\mathbf{0}, \mathbf{I})$
-

sign of the projection, ensuring that similar vectors yield similar hash values. For $i \in \{1, \dots, k\}$, the seed and the noise for patch i are:

$$s_i = \text{hash}(\text{sign}(\langle \mathbf{v}, \mathbf{r}_1^i \rangle), \dots, \text{sign}(\langle \mathbf{v}, \mathbf{r}_b^i \rangle), i, \text{salt}).$$

$$\mathbf{z}_i \stackrel{s_i}{\sim} \mathcal{N}(\mathbf{0}, \mathbf{I})$$

Having repetitive patches in the initial noise may distort image generation. Therefore, we include the patch index in the hash function input to ensure that $s_i \neq s_j$ even when the input bits are identical (see Figure 8 for a visualization of what happens to the noise without the patch-dependent input). For cryptographic security, we also hash a secret salt.

Watermark Generation

Algorithm 2 Watermark Generation

- 1: **Input:** prompt: text prompt, n : number of patches, b : number of bits, salt: secret salt
 - 2: **Output:** Watermarked image of prompt
 - 3: $\mathbf{z}^{\text{pre}} \sim \mathcal{N}(\mathbf{0}, \mathbf{I})$
 - 4: $\mathbf{x}^{\text{pre}} \leftarrow \text{Diffusion}(\mathbf{z}^{\text{pre}}, \text{prompt})$
 - 5: $\mathbf{v} \leftarrow \text{Embed}(\text{Caption}(\mathbf{x}^{\text{pre}}))$
 - 6: **for** $i = 1, \dots, n$ **do**
 - 7: $\mathbf{z}_i \leftarrow \text{SimHash}(\mathbf{v}, i, \text{salt})$
 - 8: **end for**
 - 9: **return** $\text{Diffusion}(\mathbf{z}, \text{prompt})$
-

The first step of the generation process is to find a semantic vector describing the image that will be generated. Ideally, the semantic vector depends only on the prompt and correlates exclusively with images generated from it. Yet, in practice, predicting the image semantics based on the prompt is difficult.

Our solution begins by generating a proxy image \mathbf{x}^{pre} . Then, we use a captioning model to achieve a text description

of the generated image. The caption is embedded into a latent semantic space, resulting in a semantic vector \mathbf{v} , which captures the high-level semantics of the generated image by the prompt. Next, we generate the watermarked noise \mathbf{z} in patches using the semantic vector \mathbf{v} and SimHash. Finally, we apply diffusion to the watermarked initial noise.

Embedding Optimization. During detection, the generated image will be captioned to obtain a semantic vector $\tilde{\mathbf{v}}$. To make sure that \mathbf{v} correlates to $\tilde{\mathbf{v}}$ and not to unrelated vectors, we fine-tune the embedding model to improve the similarity between the embedding of different images generated from the same prompt.

Algorithm 3 Watermark Detection

```

1: Input:  $\tilde{\mathbf{x}}$ : suspect image,  $\tau$ : patch distance threshold,  $n$ : number of patches,  $m^{\text{match}}$ : match threshold,  $b$ : number of bits, salt: secret salt
2: Output: Watermark detection (True/False)
3:  $\tilde{\mathbf{v}} \leftarrow \text{Embed}(\text{Caption}(\tilde{\mathbf{x}}))$ 
4:  $\mathbf{z}^{\text{inv}} \leftarrow \text{InverseDiffusion}(\tilde{\mathbf{x}})$ 
5:  $m \leftarrow 0$ 
6: for  $i = 1, \dots, n$  do
7:    $\tilde{\mathbf{z}}_i \leftarrow \text{SimHash}(\tilde{\mathbf{v}}, i, \text{salt})$ 
8:   if  $\|\tilde{\mathbf{z}}_i - \mathbf{z}_i^{\text{inv}}\|_2 < \tau$  then
9:      $m \leftarrow m + 1$ 
10:  end if
11: end for
12: return  $m \geq m^{\text{match}}$ 

```

Watermark Detection

For detection, we generate noise based on the semantic content of the image and check how well it corresponds to the reconstructed noise obtained through DDIM inversion (Algorithm 3). We begin by embedding the image to get a semantic vector $\tilde{\mathbf{v}}$ that captures the content of the image. SimHash is then applied to this vector as in the watermark generation process, generating an estimated initial noise $\tilde{\mathbf{z}}$. Finally, we use inverse diffusion (e.g., DDIM [23]) to approximately reconstruct the initial noise \mathbf{z}^{inv} from the image.

Since \mathbf{v} and $\tilde{\mathbf{v}}$ may differ, \mathbf{z} and $\tilde{\mathbf{z}}$ are not necessarily the same. However, by the similarity property of SimHash, \mathbf{z} and $\tilde{\mathbf{z}}$ will be identical on some patches as long as \mathbf{v} and $\tilde{\mathbf{v}}$ are close. On the patches i where $\tilde{\mathbf{z}}_i = \mathbf{z}_i$,

$$\|\tilde{\mathbf{z}}_i - \mathbf{z}_i^{\text{inv}}\|_2 = \|\mathbf{z}_i - \mathbf{z}_i^{\text{inv}}\|_2. \quad (1)$$

For such i , the only error stems from the diffusion and inverse diffusion processes. Empirically, we find that there is a threshold τ so that two patches have ℓ_2 -norm difference at most τ it is likely that they were generated from the same random seed.

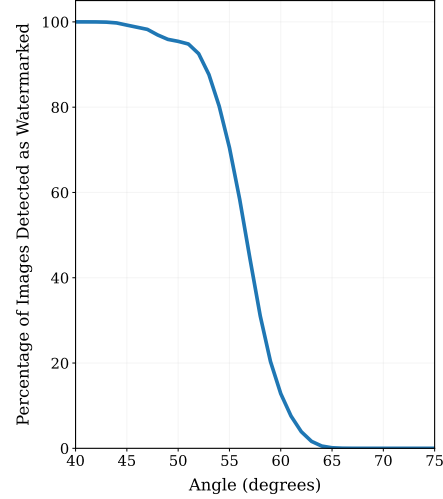


Figure 4. **Watermark Detection vs. Semantic Similarity.** We plot the empirical probability of declaring an image as watermarked as a function of the angle between the semantic embedding used for watermark generation ($n = 1024$ and $b = 7$) and that of the inspected image. Our use of locally-sensitive hashing allows us to constrain the semantic embedding of the image we deem watermarked according to the initial noise used.

Semantic Similarity Detection. In order to detect whether an image was initially generated with our watermark, we count the number of patches that *match* (i.e., their ℓ_2 -norm distance is at most τ). If the number of matches is above a set threshold n^{match} then we declare the image is watermarked. In Section 3.3, we analyze the probability of correctly identifying a watermarked image.

Tampering Detection. In addition to the association between the watermark and the semantic embedding, edits such as object addition, removal, or modification are likely to alter the estimated initial noise in the affected image regions. This enables our watermark to provide localized information about edits that might have been made to the image. Consequently, even if the semantic embedding $\tilde{\mathbf{v}}$ aligns well with the initial embedding \mathbf{v} after edits, such tampering can still be detected by identifying localized patches in the reconstructed initial noise that neither match the expected noise nor any other valid input to the hash function. Inspecting the patches one by one, the model owner may recover the b input bits for each patch with an exhaustive search over the 2^b options per patch, and recover a matching initial noise.

Comparing this reconstructed noise to the inverted noise \mathbf{z}^{inv} allows us to detect which patches may have been modified. The total time for this search scales as $n \cdot 2^b$ (which is much faster than naively searching over all $2^{(b \cdot n)}$ possible initial noise). After obtaining a per patch map (see Figure 3b), we may apply a *spatial test* as the one described

in Section 10.

In any case, the local patch inspection is only required when an image is deemed watermarked by semantic similarity detection; but the watermark owner would like to have a finer understanding of the edits that might have been applied to it. This inspection is especially useful against the CAT ATTACK, described in Section 4.

3.3. Analysis

Before formally analyzing our watermarking scheme, we state a simplifying assumption on the distance between the initial and reconstructed noise patches. We assume the noise patches are close if and only if the suspect image was produced from the same noise as the one given by our watermarking scheme. The impact of low-likelihood events, where unrelated patches end up close after noise reconstruction, remains part of our empirical analysis in Section 5.

Assumption 3.1 (Patch Distance Separation). *There is a threshold τ^{dist} so that, for all generation noises \mathbf{z} , inverted noises \mathbf{z}^{inv} , and patches $i \in [k]$,*

$$\|\mathbf{z}_i - \mathbf{z}_i^{\text{inv}}\|_2 \leq \tau^{\text{dist}}$$

if and only if $\mathbf{z}^{\text{inv}} = \text{InverseDiffusion}(\text{Diffusion}(\mathbf{z}))$.

An immediate consequence of the patch distance separation assumption is that we never declare an image as watermarked if its initial noise was not generated using our watermarking scheme. In practice, such unrelated images can match with a few patches; however, it is highly unlikely for them to match with the n^{match} needed for our method to declare a detection.

Unrelated prompts. A key property of our watermarking approach is its resistance to forgeries generated from unrelated prompts. Prior watermarking methods declare an image as watermarked as long as the pattern is embedded in the initial noise and the diffusion and inverse diffusion processes remain reasonably accurate. However, this creates vulnerabilities - an adversary could take an existing watermark and apply it to an unrelated, potentially offensive, or misleading prompt.

In contrast, our approach strengthens watermark integrity by requiring that the new prompt remains semantically close to the original. This ensures that watermarks are not erroneously detected in entirely unrelated images.

Lemma 3.2 (Detection Probability). *Consider a suspect image $\tilde{\mathbf{x}}$ produced from our watermarking scheme with initial semantic vector \mathbf{v} . Let $\tilde{\mathbf{v}}$ be the (possibly quite different) semantic embedding of $\tilde{\mathbf{x}}$, and $\theta \in [-90^\circ, 90^\circ]$ be the angle between \mathbf{v} and $\tilde{\mathbf{v}}$. Set θ^{mid} as the threshold between related*

Table 1. **Watermark Detection Probabilities.** Example detection probabilities for suspect images generated by our watermarking scheme with an angle threshold of $\theta^{\text{mid}} = 70^\circ$, $n = 1024$ patches, and $b = 4$ bits. For images with angles deviating by more than 5° from the threshold, our method distinguishes between related and unrelated watermarked images.

Semantic Angle: $\theta(\mathbf{v}, \tilde{\mathbf{v}})$	Detection Probability
80	3.06×10^{-6}
75	0.0111
70	0.507
65	0.992
60	1.0

and unrelated semantic vectors. The probability that we identify the image as watermarked is

$$\sum_{k=\lfloor n\rho(\theta^{\text{mid}}) \rfloor}^n \binom{n}{k} \rho(\theta)^k (1 - \rho(\theta))^{n-k}. \quad (2)$$

where $\rho(\theta) = \left(1 - \frac{\theta}{180^\circ}\right)^b$.

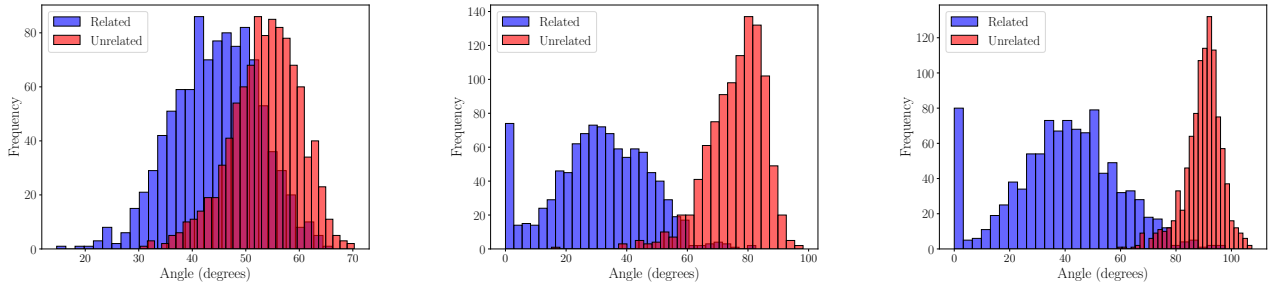
We illustrate in the example below the sharp detection thresholds Lemma 3.2 implies; specifically how watermark detection probability varies with semantic similarity between the original and a potentially modified image. We delay the proof of Lemma 3.2 to the appendix.

Example 3.3 (Sharp Detection Thresholds). *Our watermarking scheme embeds a semantic vector \mathbf{v} into an image at generation time. When evaluating a suspect image that was generated via our watermark, we extract its current semantic vector $\tilde{\mathbf{v}}$. The probability of a watermark detection depends on the semantic angle $\theta(\mathbf{v}, \tilde{\mathbf{v}})$ between \mathbf{v} and $\tilde{\mathbf{v}}$.*

For instance, Figure 5c illustrates a separation between vectors associated with the original image and those that are unrelated, occurring at a threshold of approximately $\theta^{\text{mid}} \approx 70^\circ$. When our watermarking scheme is run with $\theta^{\text{mid}} = 70^\circ$, $n = 1024$, and $b = 4$, Table 1 quantifies the probability of a watermark detection. For images with angles beyond 5° of the threshold, we almost always correctly distinguish between related and unrelated watermarked images (under assumption 3.1; see Figure 4 for the empirical curve).

4. The CAT ATTACK- Harmful Image Edits

Commonly evaluated forgery attacks typically aim to forge the entire image. The forged image in that case may have no semantic connection to the image (or group of images) from which the watermark was stolen. Yet, even when such attacks are not possible, the model owner’s security might still be compromised. Here, we explore one such case, where the attacker locally modifies an existing watermarked image. Adding new content to a watermarked image may pose



(a) **Image Feature Vector.** Direct use of image feature embedding fails to separate related from unrelated images.

(b) **Caption Embeddings.** Employing caption embeddings from *blip2-flan-t5-xl* and *paraphrase-mpnet-base-v2* yields improved separation.

(c) **Fine-tuned Caption Embeddings.** Fine-tuning the embedding model on 10k caption pairs further enhances separation.

Figure 5. **Ablation of Embedding Strategies for Watermark Detection.** Comparison of angle separation between related and unrelated images using different embedding approaches. The raw image feature vector (left) fails to distinguish semantic relationships, while caption embeddings (center) substantially improve separation. Fine-tuning the embedding model (right) yields additional gains in detection accuracy.

reputational risks to the model owner, even if the rest of the image remains unchanged. Such editing attacks are expected to be most effective against watermarks that are relatively resilient to *removal attacks* - a watermark that is removed after small edits will typically be removed even after edits that do not change the content.

Here, we consider an attack where a cropped object is pasted into a watermarked image. We refer to it as the CAT ATTACK. Our watermark method can detect such edits, and declare the image non-watermarked (or watermarked and edited) in two different ways: global *Semantic Similarity Detection* and local *Tampering Detection* (both described in Section 3). In practice, we recommend starting with Semantic Similarity Detection as a faster approach that would catch most conventional attacks. When further inspection is needed, a more local *Tampering Detection* can be used.

5. Empirical Analysis

In this section, we evaluate the robustness of SEAL.

Setting. To ensure a fair comparison with prior work [4, 7, 25], we use Stable Diffusion-v2 [20] with 50 inference steps for both generation and inversion for all methods. Evaluations were conducted on a set of prompts sourced from [21]. We set $n = 1024$ and $b = 7$ for all experiments. An ablation study on the effects of n and b is available in Section 11.

Regeneration with the Private Model. Prior works assume that the attacker lacks access to the model weights (which are needed for accurate DDIM noise inversion) and that the noise used during generation cannot be forged or approximated with sufficient accuracy. Going beyond previous studies, we consider here a more challenging scenario in which the attacker has full access to the model weights

and can invert the generated image using the same model that produced it. The attacker’s access to the private model is taken as an upper bound for the attacker’s capability in a forgery attack [4, 17].

In our experiment, we first generate an image using watermarked noise. We then perform an inversion with the same model to recover an approximate initial noise, which is subsequently used to generate a second image. Because the attack prompt differs from the original prompt, the semantic embedding of the image $\tilde{\mathbf{v}}$ changes to \mathbf{v}_{attack} . The detection algorithm, therefore compares the estimated noise to a reference derived from \mathbf{v}_{attack} (and not $\tilde{\mathbf{v}}$). The noise based on \mathbf{v}_{attack} is less likely to correlate to the pattern embedded in the image, enabling the detection algorithm to declare the image as ‘not watermarked’ and evade the attack. As can be seen in Table 3, our method uniquely provides non-trivial robustness in this setting.

Cat Attack. In this experiment, we explore the resilience of our watermarking method by pasting a cat image onto a watermarked image. The cat image is randomly resized to between 30% and 60% of the watermarked image’s dimensions and placed at a random location, as exemplified in Figure 3a (We use here a cat to avoid dealing with not-safe-for-work material). Unlike previous watermarking techniques, which overlook semantic content and thus fail to detect such alterations, our approach identifies modifications by observing elevated ℓ_2 norms in the patches where the cat is overlaid, as shown in Figure 3b. However, since our method hinges on counting patches with an ℓ_2 similarity to the reference pattern norm below a given threshold, it may occasionally miss these changes.

To increase our robustness to such attacks, we use the *Tampering Detection* technique detailed in Section 3. The results in Table 2 reveal that, while our method offers some

Table 2. **Detection AUC Under the Cat Attack.** AUC of detecting edits in generated images, as described in Section 4.

Method	AUC
WIND	0.000
Tree-Ring	0.000
Gaussian Shading	0.000
SEAL	0.551
SEAL+ Spatial Test	0.982

Table 3. **Robustness to Private Model-Based Regeneration Attack.** An attacker with access to the private model weights can approximate the watermarked initial noise by inverting a watermarked image using the private model. We evaluate how accurately different methods evade the false identification of unrelated images, generated with this initial noise, as watermarked.

Method	AUC
WIND	0.000
Tree-Ring	0.000
Gaussian Shading	0.000
SEAL	0.708

robustness even without the spatial test, integrating it significantly improves detection. Other methods are vulnerable to this type of attack, as they strive not to be easily removed by small edits. Since our robustness here is in tension with our resistance to watermark removal attacks, we next analyze our method performance against these types of attacks.

Image Transformation Attacks. We evaluated the robustness of SEAL under a standard suite of image transformations (see Section 12). As shown in Figure 6, SEAL achieves an average detection rate of 0.896 under these conditions. This is comparable to some watermarking and somewhat lower than others [25]. Yet, our method is uniquely resistant to forgery. Further enhancements, such as incorporating rotation search or sliding-window search during detection, could improve its robustness against removal.

Ablation of Captioning and Embedding Models. A straightforward approach for our method would be to use the feature vector from the first generated image rather than the embedding of its caption. However, as illustrated in Figure 5a, this approach fails to yield a clear separation between related and unrelated images. Consequently, we employ the *blip2-flan-t5-xl* [15] model for caption generation and the *paraphrase-mpnet-base-v2* [19] for deriving caption embeddings, which results in a more distinct separation as shown in Figure 5. To further enhance our method’s accuracy, we fine-tuned the embedding model using 10k pairs of related

captions, leading to additional improvements (Figure 5c¹).

Steganalysis Attack. We evaluate the robustness of our method against a steganalysis attack [26] that attempts to approximate the watermark by subtracting non-watermarked images from watermarked ones. As shown in App. Table 4, SEAL maintains high performance under this attack.

Generation Quality. Our method is distortion-free at the single-image level, as the noise is drawn from a pseudo-random Gaussian distribution. Consequently, all single-image quality metrics are identical to those of non-watermarked images (see also Section 14).

6. Limitation and Discussion

Stronger Forgery Attacks. Although we evaluated a stronger set of forgery attacks compared to prior work, other types of forgery attacks might still potentially compromise our watermark. For example, a highly persistent attacker might attempt to gather information about the correlation between individual initial noise patches and the image semantics. While not theoretically impossible, an attacker would face several practical limitations in carrying out such an attack. Among them, are the lack of access to the private model weights, the inherent stochasticity of the watermark, and the watermark owner’s ability to deploy multiple instances of the hash function.

Attacker Advantage and Removal Attacks. Our method is more vulnerable to removal attacks than some existing methods. However, we believe that a sufficiently persistent attacker can remove most current watermarks. Nonetheless, increasing the robustness of watermarks holds significant societal value. It helps reduce misleading content and makes forgery attacks more difficult, which is crucial for their practical deployment.

Additional limitations and discussion points can be found in Section 13.

7. Conclusion

We introduce the first initial noise-based watermarking method for diffusion models that is both database-free and semantic-aware. Our suggested watermark is uniquely robust against a new class of stronger forgery attacks. We hope our work highlights the potential of semantic-aware watermarking and helps pave the way forward for further research in this area.

¹To facilitate reproducibility and encourage further research, we made our fine-tuned caption embedding model publicly available at <https://huggingface.co/kasraarabi/finetuned-caption-embedding>

References

- [1] Ali Al-Haj. Combined dwt-dct digital image watermarking. *Journal of computer science*, 3(9):740–746, 2007. 1
- [2] Bang An, Mucong Ding, Tahseen Rabbani, Aakriti Agrawal, Yuancheng Xu, Chenghao Deng, Sicheng Zhu, Abdirisak Mohamed, Yuxin Wen, Tom Goldstein, et al. Waves: Benchmarking the robustness of image watermarks. *arXiv preprint arXiv:2401.08573*, 2024. 2
- [3] Alexandr Andoni and Piotr Indyk. Near-optimal hashing algorithms for approximate nearest neighbor in high dimensions. *Communications of the ACM*, 51(1):117–122, 2008. 3
- [4] Kasra Arabi, Benjamin Feuer, R Teal Witter, Chinmay Hegde, and Niv Cohen. Hidden in the noise: Two-stage robust watermarking for images. *arXiv preprint arXiv:2412.04653*, 2024. 1, 2, 7
- [5] Charlotte Bird, Eddie Ungless, and Atoosa Kasirzadeh. Typology of risks of generative text-to-image models. In *Proceedings of the 2023 AAAI/ACM Conference on AI, Ethics, and Society*, pages 396–410, 2023. 1, 3
- [6] Moses S Charikar. Similarity estimation techniques from rounding algorithms. In *Proceedings of the thirty-fourth annual ACM symposium on Theory of computing*, pages 380–388, 2002. 4, 1
- [7] Hai Ci, Pei Yang, Yiren Song, and Mike Zheng Shou. Ringid: Rethinking tree-ring watermarking for enhanced multi-key identification. In *European Conference on Computer Vision*, pages 338–354. Springer, 2024. 2, 7
- [8] Mayur Datar, Nicole Immorlica, Piotr Indyk, and Vahab S Mirrokni. Locality-sensitive hashing scheme based on p-stable distributions. In *Proceedings of the twentieth annual symposium on Computational geometry*, pages 253–262, 2004. 3
- [9] Pierre Fernandez, Alexandre Sablayrolles, Teddy Furon, Hervé Jégou, and Matthijs Douze. Watermarking images in self-supervised latent spaces. In *ICASSP 2022-2022 IEEE International Conference on Acoustics, Speech and Signal Processing (ICASSP)*, pages 3054–3058. IEEE, 2022. 1
- [10] Pierre Fernandez, Guillaume Couairon, Hervé Jégou, Matthijs Douze, and Teddy Furon. The stable signature: Rooting watermarks in latent diffusion models. In *Proceedings of the IEEE/CVF International Conference on Computer Vision*, pages 22466–22477, 2023. 2
- [11] Aristides Gionis, Piotr Indyk, Rajeev Motwani, et al. Similarity search in high dimensions via hashing. In *Vldb*, pages 518–529, 1999. 2
- [12] Sam Gunn, Xuandong Zhao, and Dawn Song. An undetectable watermark for generative image models. *arXiv preprint arXiv:2410.07369*, 2024. 2
- [13] Piotr Indyk and Rajeev Motwani. Approximate nearest neighbors: towards removing the curse of dimensionality. In *Proceedings of the thirtieth annual ACM symposium on Theory of computing*, pages 604–613, 1998. 2
- [14] Kokil Jaidka, Tshuhan Chen, Simon Chesterman, Wynne Hsu, Min-Yen Kan, Mohan Kankanhalli, Mong Li Lee, Gyula Seres, Terence Sim, Araz Taeihagh, et al. Misinformation, disinformation, and generative ai: Implications for perception and policy. *Digital Government: Research and Practice*, 6(1):1–15, 2025. 1
- [15] Junnan Li, Dongxu Li, Silvio Savarese, and Steven Hoi. Blip-2: Bootstrapping language-image pre-training with frozen image encoders and large language models. In *International conference on machine learning*, pages 19730–19742. PMLR, 2023. 8
- [16] Tsung-Yi Lin, Michael Maire, Serge Belongie, James Hays, Pietro Perona, Deva Ramanan, Piotr Dollár, and C Lawrence Zitnick. Microsoft coco: Common objects in context. In *Computer vision—ECCV 2014: 13th European conference, Zurich, Switzerland, September 6–12, 2014, proceedings, part v 13*, pages 740–755. Springer, 2014. 3
- [17] Andreas Müller, Denis Lukovnikov, Jonas Thietke, Asja Fischer, and Erwin Quiring. Black-box forgery attacks on semantic watermarks for diffusion models. *arXiv preprint arXiv:2412.03283*, 2024. 7
- [18] KA Navas, Mathews Cheriyan Ajay, M Lekshmi, Tampy S Archana, and M Sasikumar. Dwt-dct-svd based watermarking. In *2008 3rd international conference on communication systems software and middleware and workshops (COMSWARE'08)*, pages 271–274. IEEE, 2008. 1
- [19] Nils Reimers and Iryna Gurevych. Sentence-bert: Sentence embeddings using siamese bert-networks. In *Proceedings of the 2019 Conference on Empirical Methods in Natural Language Processing*. Association for Computational Linguistics, 2019. 8
- [20] Robin Rombach, Andreas Blattmann, Dominik Lorenz, Patrick Esser, and Björn Ommer. High-resolution image synthesis with latent diffusion models. In *Proceedings of the IEEE/CVF conference on computer vision and pattern recognition*, pages 10684–10695, 2022. 7
- [21] Gustavo Santana. Stable-diffusion-prompts. <https://huggingface.co/datasets/Gustavosta/Stable-Diffusion-Prompts>, 2024. Accessed: 2024-11-20. 7, 3
- [22] Irene Solaiman, Zeerak Talat, William Agnew, Lama Ahmad, Dylan Baker, Su Lin Blodgett, Canyu Chen, Hal Daumé III, Jesse Dodge, Isabella Duan, et al. Evaluating the social impact of generative ai systems in systems and society. *arXiv preprint arXiv:2306.05949*, 2023. 1
- [23] Jiaming Song, Chenlin Meng, and Stefano Ermon. Denoising diffusion implicit models. *arXiv preprint arXiv:2010.02502*, 2020. 2, 5
- [24] Matthew Tancik, Ben Mildenhall, and Ren Ng. Stegastamp: Invisible hyperlinks in physical photographs. In *Proceedings of the IEEE/CVF conference on computer vision and pattern recognition*, pages 2117–2126, 2020. 1
- [25] Yuxin Wen, John Kirchenbauer, Jonas Geiping, and Tom Goldstein. Tree-ring watermarks: Fingerprints for diffusion images that are invisible and robust. *arXiv preprint arXiv:2305.20030*, 2023. 1, 2, 7, 8
- [26] Pei Yang, Hai Ci, Yiren Song, and Mike Zheng Shou. Steganalysis on digital watermarking: Is your defense truly impervious? *arXiv preprint arXiv:2406.09026*, 2024. 8
- [27] Zijin Yang, Kai Zeng, Kejiang Chen, Han Fang, Weiming Zhang, and Nenghai Yu. Gaussian shading: Provable

performance-lossless image watermarking for diffusion models. In *Proceedings of the IEEE/CVF Conference on Computer Vision and Pattern Recognition*, pages 12162–12171, 2024. [1](#), [2](#)

- [28] Xuandong Zhao, Kexun Zhang, Zihao Su, Saastha Vasani, Ilya Grishchenko, Christopher Kruegel, Giovanni Vigna, Yu-Xiang Wang, and Lei Li. Invisible image watermarks are provably removable using generative ai. *Advances in Neural Information Processing Systems*, 37:8643–8672, 2025. [2](#), [1](#)
- [29] Jiren Zhu, Russell Kaplan, Justin Johnson, and Li Fei-Fei. Hidden: Hiding data with deep networks. In *Proceedings of the European conference on computer vision (ECCV)*, pages 657–672, 2018. [1](#)

SEAL: Semantic Aware Image Watermarking

Supplementary Material

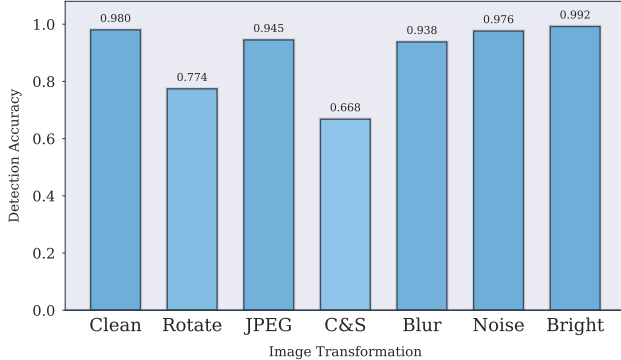


Figure 6. **Robustness of Watermark Detection Against Image Transformations.** Comparison of correct watermark detection accuracy of SEAL under various image transformations.

8. Additional Related Works

Post-Processing Methods. Post-processing techniques embed watermarks after the image generation stage, providing model-agnostic flexibility at the cost of potential quality degradation. Frequency-domain methods, such as methods using the Discrete Wavelet Transform (DWT) and Discrete Cosine Transform (DCT) [1, 18], embed watermarks in the transformed domains and offer robustness against operations like resizing and translation. Complementing these, deep encoder-decoder frameworks such as HiDDeN [29] and StegaStamp [24] utilize end-to-end neural training for watermark embedding and extraction. Despite these advancements, however, these methods are vulnerable to regeneration attacks [28]. Alternative strategies operating in latent spaces have also been proposed [9], though they also remain susceptible to sophisticated removal attacks.

9. Proof of Lemma 3.2

Proof of Lemma 3.2. The angle between the original semantic vector \mathbf{v} used to generate the watermark and extracted semantic vector $\tilde{\mathbf{v}}$ of the suspect image is

$$\theta(\mathbf{v}, \tilde{\mathbf{v}}) = \cos^{-1} \left(\frac{\langle \mathbf{v}, \tilde{\mathbf{v}} \rangle}{\|\mathbf{v}\|_2 \|\tilde{\mathbf{v}}\|_2} \right) \in [-90^\circ, 90^\circ].$$

By the property of SimHash² and Assumption 3.1, the

²See Section 3 of [6] for details on why

$$\Pr_{\mathbf{r} \sim \mathcal{N}(\mathbf{0}, \mathbf{I})} (\text{sign}(\langle \mathbf{v}, \mathbf{r} \rangle) = \text{sign}(\langle \tilde{\mathbf{v}}, \mathbf{r} \rangle)) = 1 - \frac{\theta}{180^\circ}. \quad (3)$$

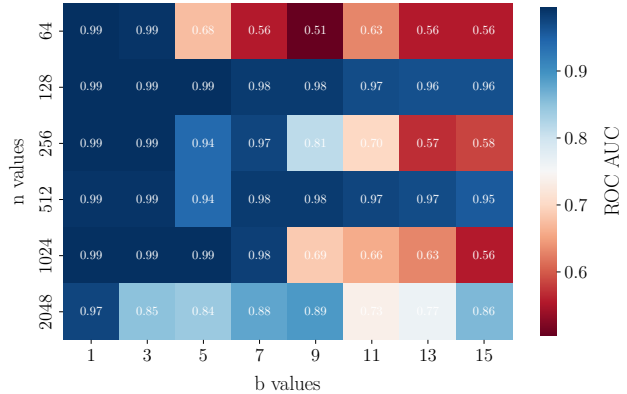


Figure 7. **Ablation Study of the Number of Patches (n) and Bits (b) on Watermark Detection Performance.**

probability³ that the i th patch aligns is

$$\rho(\theta) := \Pr(\|\mathbf{z}_i - \tilde{\mathbf{z}}_i\|_2 \leq \tau) = \left(1 - \frac{\theta}{180^\circ}\right)^b.$$

Since each SimHash instance is independent, the number of matches m is distributed like a Binomial with n trials and success probability $\rho(\theta)$. During watermark detection, we count the number of patches that match, declaring an image watermarked if the number of matches exceeds the threshold m^{match} . Setting $m^{\text{match}} = \lfloor n\rho(\theta^{\text{mid}}) \rfloor$ yields the lemma statement. \square

10. Spatial Test

To better analyze potential image tampering, we examine the structural organization of high-intensity regions in the patch correspondence heatmaps (see Section 3, Tampering Detection). Specifically, we threshold the heatmap data at the 80th percentile and identify connected components. The extracted parameter, the number of distinct clusters detected at this threshold, provides insight into the fragmentation of high-intensity regions. A higher number of clusters indicates a more dispersed distribution, while a lower number suggests more contiguous structures, which may be indicative of image tampering.

11. Ablation of Number of Patches and Bits.

To investigate the impact of the number of patches (n) and the number of bits (b) used to generate the initial noise, we

³Technically, there is an additional chance of a random collision but, given the size of modern cryptographic hash functions like SHA2, we assume this probability is negligible.

Table 4. **Robustness of Steganalysis-Based Removal.** Comparison of performance metrics (AUC for SEAL, Tree-Ring, and, WIND and bit accuracy for Gaussian Shading) under various levels of averaging.

Method	5	10	20	50	100	200	500	1000	2000	5000
Gaussian Shading (Bit Acc)	0.490	0.469	0.537	0.488	0.486	0.479	0.461	0.463	0.465	0.462
Tree-Ring (AUC)	0.293	0.267	0.314	0.275	0.214	0.228	0.211	0.224	0.224	0.241
WIND (AUC)	1.000	1.000	1.000	1.000	1.000	1.000	1.000	1.000	1.000	1.000
SEAL (AUC)	1.000	1.000	1.000	1.000	1.000	1.000	1.000	1.000	1.000	1.000

conducted an exhaustive ablation study across various parameter combinations. The results are presented in Figure 7.

12. Transformations for the Removal Attack

We use a standard suit of transformations, including a 75° rotation, 25% JPEG compression, 75% random cropping and scaling (C & S), Gaussian blur using an 8×8 filter, Gaussian noise with $\sigma = 0.1$, and color jitter with a brightness factor uniformly sampled between 0 and 6.

13. Additional Limitations and Discussion

Distortion-Free Property for Sets of Images Our watermarking scheme securely generates the noise for each patch from a normal distribution, ensuring that each individual noise is distributed from a normal distribution. However, multiple watermarked images corresponding to related prompts may leak information about the noise i.e., the noise in some patches will match while the noise in other patches does not. This leakage arises from our design choice to make similar prompts produce similar watermarks, a feature that enhances consistency but comes at the cost of some information exposure.

In contrast, some prior works do not exhibit this property and instead maintain a stronger sense of distribution-free randomness. Ignoring cases where the exact same noise is reused, such as when multiple images are generated by the same user in [27], these methods ensure that each image is independently sampled from a normal distribution. This fundamental difference highlights a trade-off between ensuring independent randomness and enabling structured watermark consistency across related prompts. A user concerned about the distortion-free property for sets may vary the secret salt for different generations. This will allow the user to enjoy the best of both worlds, At the cost of searching through possible salts that may have been used during detection time.

Further Possible Improvement. We made an initial attempt to find a semantic vector that is both known before generation and recoverable from the generated image. Yet, we believe this is a promising direction for future research. Improved semantic embedding methods, as well as approaches

that jointly optimize image generation and semantic descriptor generation, could enhance the correspondence between the embedded watermark and the image’s semantics. Such advancements may enable much stricter bounds on detecting when a watermarked image has been tampered with and how.

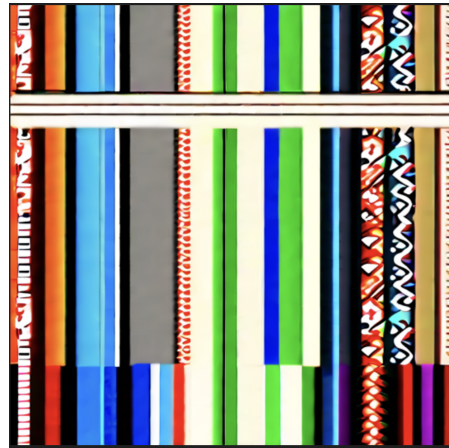


Figure 8. **Impact of Repetitive Patches in the Initial Noise on Image Generation.**

14. Image Quality Results

Table 5. **CLIP Score Evaluation.** Comparison of CLIP scores before and after watermarking for images generated using prompts from the Stable-Diffusion-Prompts [21] and COCO [16] dataset.

Stable-Diffusion-Prompts		COCO	
CLIP (before)	CLIP (after)	CLIP (before)	CLIP (after)
32.378	32.401	31.365	31.499

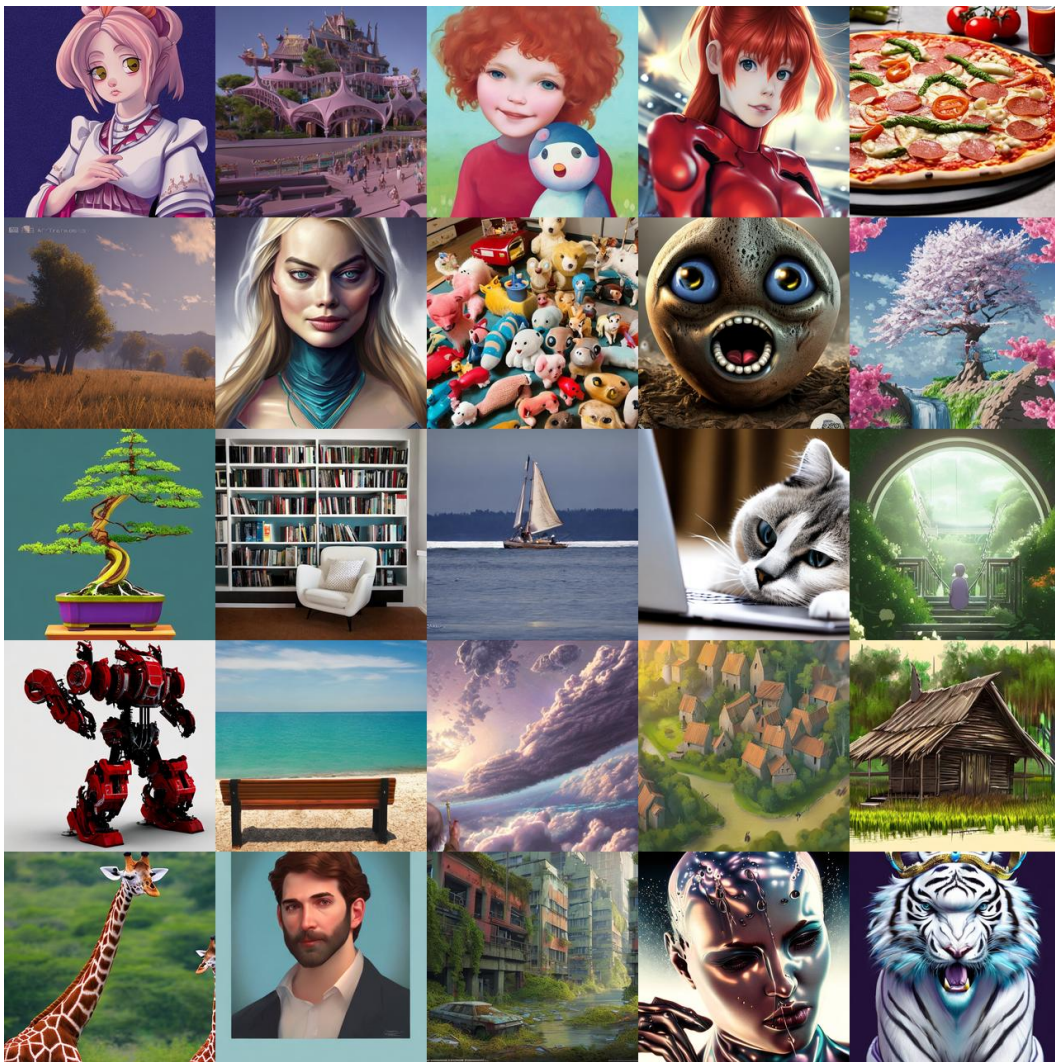


Figure 9. **Watermarked images generated using SEAL.**